Biochimica et Biophysica Acta, 934 (1988) 314–328
Elsevier

BBA 42810

Flash-induced H^+ binding by bacterial photosynthetic reaction centers: comparison of spectrophotometric and conductimetric methods

Péter Maróti * and Colin A. Wraight

Department of Physiology and Biophysics and Department of Plant Biology, University of Illinois, Urbana, IL (U.S.A.)

(Received 21 December 1987)

Key words: Bacterial photosynthesis; Reaction center; Proton binding; Electric conductance change; pH indicator dye; (*Rb. sphaeroides*)

H^+ binding following flash excitation of isolated reaction centers from *Rhodobacter sphaeroides* was measured using a conductimetric method. A procedure is described for calibrating the H^+ change and the method is compared to the more widely used spectrophotometric assay of pH-indicator dyes. The two methods agree extremely well and confirm a severe paradox in the pH dependence of the H^+ binding stoichiometry – that reaction centers in the light-activated, charge-separation state, $P^+(Q_AQ_B)^-$, fail to bind net protons at pH values near neutral or lower, although proton binding is seen at higher pH. This is in contrast to expectations arising from the equilibrium redox behavior of the acceptor quinones, Q_A and Q_B, and with the pH dependence of the one-electron equilibrium between $Q_A^-Q_B$ and $Q_AQ_B^-$. The observed proton binding is discussed in terms of multiple protonation equilibria linked to the redox states of the acceptor quinones and of the primary donor.

Introduction

The electron-acceptor complex of the reaction center (RC) from purple photosynthetic bacteria (Rhodospirillaceae) and of Photosystem II of oxygenic organisms consists of two quinones (Q_A and Q_B) which act in series as a two electron gate [1]. Some mechanistic details of the gate have been established for the bacterium, *Rhodobacter sphaeroides*, using isolated reaction centers [1–4]. In the absence of electron donors to the oxidized primary photoelectron donor, P^+, the light-induced charge separation recombines in a time that is sensitive to various parameters including pH [4,5] and quinone concentration [5,6]. We proposed that the observed back-reaction (reappearance of P) could be described by the following scheme [2,6]:

$$PQ_AQ_B \underset{k_0}{\overset{h\nu}{\rightleftarrows}} P^+Q_A^-Q_B \underset{k_{-2}}{\overset{k_2}{\leftrightarrow}} P^+Q_AQ_B^-$$

and that the back-reaction kinetics reflected the one-electron equilibrium ($K_2 = k_2/k_{-2}$) between Q_A and Q_B:

$$t_{1/2}(\text{obs}) = t_{1/2}^{Q_A}(1 + K_2)$$

where $t_{1/2}^{Q_A}$ is the half-time for recombination when only Q_A is functioning. This was strongly supported by Wraight and Stein [7] and has since been convincingly confirmed by Kleinfeld et al. [4].

* Permanent address: Institute of Biophysics, József Attila University, Szeged, Egyetem u.2, Hungary.

Abbreviations: RC, reaction center; LDAO, lauryldimethylamine *N*-oxide.

Correspondence: C.A. Wraight, Department of Physiology and Biophysics and Department of Plant Biology, University of Illinois, 289 Morrill Hall, 505 S. Goodwin Avenue, Urbana, IL 61801, U.S.A.

The back-reaction kinetics ($t_{1/2}$(obs)) are pH independent up to about pH 9 but become more rapid at higher pH. This behavior can be accounted for if both of the one-electron states of the quinone complex bind a proton following a flash at pH values below 9, so that K_2 is pH independent:

$$Q_A^- Q_B(H^+) \underset{K_2}{\leftrightarrow} Q_A Q_B^-(H^+)$$

The acceleration of the back reaction at higher pH indicates that K_2 becomes pH dependent, implying that $Q_A^- Q_B$ has a pK and no longer binds H^+:

$$\begin{array}{c} H^+ \\ \downarrow \\ Q_A^- Q_B \underset{K_2}{\leftrightarrow} Q_A Q_B^-(H^+) \end{array}$$

From the pH dependence of K_2, in 10 mM NaCl, Kleinfeld et al. [4] deduced a value for the pK of $Q_A^- Q_B / Q_A^- Q_B(H^+)$ (p$K_A = 9.8$) that is identical to that obtained from redox titrations of the Q_A/Q_A^- couple in chromatophores [8]: the midpoint potential (E_m) of Q_A is pH dependent, with a slope of -60 mV/pH, from pH 5 up to the pK of the reduced species, $Q_A^-/Q_A^-(H^+)$, at pH 9.8. Our own studies in 100 mM NaCl indicated a slightly lower pK value (p$K_A = 9.6$) [5] which is also identical to the redox pK observed in 100 mM NaCl for isolated RCs incorporated in phospholipid vesicles [9]. Analysis of the back-reaction kinetics for $P^+Q_AQ_B^-$ at high pH suggested a pK for $Q_AQ_B^-/Q_AQ_B^-(H^+)$ (pK_B) of 11.3 in 10 mM NaCl [4] and somewhat below pH 11 in 100 mM NaCl [5]. The implied H^+ binding by the state $P^+Q_AQ_B^-$ is consistent with redox titrations of the Q_B/Q_B^- couple in chromatophores, for which the E_m was strongly pH dependent at least between pH 8 and 10 [10].

Studies on isolated reaction centers have shown that certain inhibitors block electron transfer from Q_A^- to Q_B by competitively displacing Q_B from a binding site in the protein [5,9,11,12]. These inhibitors, which include *o*-phenanthroline and *s*-triazines such as terbutryn or atrazine, also raise the pK of $Q_A^-/Q_A^-(H^+)$ (pK_T) to above 10 (Refs. 8, 9 and 23) (accompanying article)).

These various observations clearly lead to the expectation that net H^+ binding should accompany flash excitation of isolated RCs at neutral and slightly alkaline pH values, but should fall off as the pH is raised through the appropriate pK value of the active acceptor quinone species. In preliminary communications [13,14], we have reported that the net H^+ binding behavior, observed spectrophotometrically with pH-indicator dyes, is severely at odds with this expectation: at neutral pH, H^+ binding fails to occur, but sets in as the pH is raised. At still higher pH, the H^+ binding declines again, in accordance with the known pK values of the reduced acceptor quinone complex. Because of the unexpected nature of this result, we have undertaken to measure H^+ binding by an entirely independent method. We were inspired by a preliminary report by Marinetti [15] to use conductance measurements as a monitor of H^+ uptake and release. Here we describe this technique and demonstrate excellent agreement between it and the more conventional use of pH-indicator dyes. The paradoxical behavior of H^+ binding by isolated reaction centers is confirmed, and a preliminary interpretation is presented in terms of multiple ionizable groups on the RC protein under the dual influences of the redox states of P^+/P and Q/Q^- (where Q implies Q_A or Q_B).

Materials and Methods

Reaction centers were prepared from *Rhodobacter sphaeroides*, strain R-26, by detergent fractionation of chromatophores with lauryldimethylamine *N*-oxide (LDAO or Ammonyx-LO, from the Onyx Corp., Jersey City, NJ) and purified by $(NH_4)_2SO_4$ precipitation and by DEAE-cellulose chromatography [2]. However, RCs were eluted from the DEAE column in 150 mM NaCl, 0.1% LDAO, 10 mM Tris (pH 8.0) rather than 350 mM NaCl as erroneously stated in Ref. 2. After concentration by ultrafiltration and subsequent dialysis, the stock contained 0.03% LDAO and 1 mM Tris (pH = 8.1) and secondary acceptor activity was normally reduced to about 0.3–0.5 Q_B per RC. When desired, further extraction of Q_B was performed by washing the reaction centers on a DEAE column with 1 mM *o*-phenanthroline, 1% LDAO, 10 mM Tris (pH 8.0), as described by Okamura et al. [16]. Residual Q_B was routinely checked by the fraction of slow phase in the P^+Q^- recombination kinetics [7]. The same assay was applied to determine the extent of reconstitu-

tion of Q_B activity with ubiquinone-50 (Q-10; Sigma Chemicals, St. Louis, MO) added from a stock (20 mM) dispersed in 30% Triton X-100 by sonication. The levels obtained were routinely less than 10% Q_B after extraction and more than 90% after reconstitution of Q_B activity by 20 μM Q-10 in 0.03% Triton X-100.

Flash-induced conductance changes were measured in a cell containing two parallel platinum plates (6 mm × 7 mm each) fixed at a distance of 8 mm with the aid of a transparent plastic block. The block fitted in the bottom of a four sides clear 1 cm × 1 cm redox cuvette which could be placed into the sample holder of a home-made single-beam spectrophotometer. The measuring beam passed between the platinum plates, and the excitation flashes, from a xenon flash tube (EG&G FX200), were directed through the bottom of the cuvette by means of a short light guide, allowing simultaneous optical and electrical measurement. In order to minimize the flash-induced heat artifact, the excitation light guide was prepared from a water-filled glass tube (6 cm long). Light saturation, which was more than 97%, was routinely checked by comparing the extent of photooxidation of the reaction center by a single flash with that generated in a series of closely spaced flashes.

The platinum electrodes used for the conductance measurements were platinized in a solution of 3% chloroplatinic acid/0.03% lead acetate. The plating current was 50 mA/cm^2 and the polarity was reversed every 5 s. The black platinum coat decreased the Faraday impedance (depolarization) dramatically. Conductance changes in the sample were detected by a locally constructed a.c. Wheatstone bridge (Fig. 1). The frequency and amplitude of the driving sine wave applied to the bridge could be varied to optimize different requirements such as time resolution, polarization or signal-to-noise ratio. Typically a frequency of 1.2 kHz and amplitudes of 0.2–1.0 V were used. The signal from the bridge was fed into a differential amplifier (Tektronix 5A20N) and then into a lock-in amplifier (PAR, Model 120). Control of the whole measuring system and digitization and acquisition of data were carried out by a computer (LSI 11/73) [5]. The ability to monitor fast transients, at least to 100 kHz, with an excellent signal-to-noise ratio, is a major feature of the electronics. The ultimate limitations of the system arise from the applied frequency, the common-mode-rejection ratio of the differential amplifier and the quality factor, Q, of the lock-in amplifier.

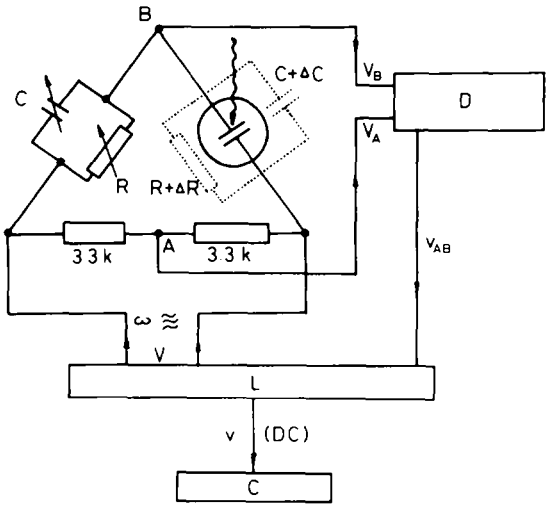

Fig. 1. Schematic of the electronics of the conductimeter. The a.c. bridge has a fixed division (1 : 1) and the measuring cell is balanced by the variable resistor (R) and capacitance (C). The exciting flash causes impedance changes in the measuring cell which can be approximated by parallel-coupled resistance (ΔR) and capacitance (ΔC) changes. The sine wave (amplitude V, frequency ω) across the bridge is shifted in phase and modified in amplitude (V_B and V_A) at the output. The differential amplifier, D, (output v_{AB}) and the lock-in amplifier, L, (output v) convert the signal from the bridge to a d.c. signal for data acquisition in the computer (C).

The sample contained approx. 1 μM reaction centers in 6 ml of 10 mM buffer. The buffers used in our experiments at different pH ranges are shown in Table I. No salt was added because the sensitivity of the conductance measurement for ion binding/unbinding is inversely related to the conductance of the sample. LDAO has a low pK (around 5) which could interfere with the H^+ binding measurements at low pH. However, the amount of LDAO carried over from the RC stock, was negligible in the sample (about 0.0003%). The final concentration of Triton was significantly higher, about 0.03–0.05%.

The sample could be stirred from the top, thereby allowing fast and uniform mixings of small amounts of externally added materials necessary for calibration or for pH adjustment. The

TABLE I

CATEGORIZATION OF BUFFERS USED IN PROTON-BINDING CONDUCTANCE MEASUREMENTS BASED ON THEIR BEHAVIOR UPON DEPROTONATION

Bistris, 2-[bis(2-hydroxyethyl)amino]-2-(hydroxymethyl)propane-1,3-diol; Mes, 4-morpholineethanesulfonic acid; Pipes, 1,4-piperazinediethanesulfonic acid; Mops, 4-morpholinepropanesulfonic acid; Hepes, 4-(2-hydroxyethyl)-1-piperazineethanesulfonic acid; Tricine, *N*-[2-hydroxy-1,1-bis(hydroxymethyl)ethyl]glycine; Ches, 2-[*N*-cyclohexylamino]ethanesulfonic acid; Tris, 2-amino-2-hydroxymethylpropane-1,3-diol; Caps, 3-cyclohexylamino-1-propanesulfonic acid.

Buffer types	Buffers used	pK		Typical behavior upon deprotonation	
				scheme	net gain in mobile charge
Cationic	L-Histidinemethylester		≈ 5.5		
	Piperazine		≈ 5.0		
	Bistris		6.5		
	Bistris propane	pK_1	6.8		
		pK_2	9.0		
	Tris		8.1	H^+ ↗ ⊕ → ⊖	−1
	Aminomethylpropanol		9.7		
	Ethylenediamine	pK_1	6.8		
		pK_2	9.9		
	Methylamine		10.6		
	Piperidine		11.1		
Dipolar (zwitterionic)	Mes		6.1		
	Pipes		6.8		
	Mops		7.2		
	Hepes		7.5		
	Tricine		8.1		
	Glycylglycine		8.2	H^+ ↗ (+ −) → ⊖	+1
	Ches		9.3		
	Glycine	pK_2	9.8		
	Aspartic acid	pK_2	10.0		
	Caps		10.4		
Anionic	Succinate	pK_2	5.6		
	Phosphate	pK_2	7.2	H^+ ↗ ⊖ → (− −)	+1
		pK_3	12.3		

anaerobic redox cuvette was continuously flushed with argon gas and was equipped with additional Pt and pH electrodes, enabling continuous monitoring of pH and E_h of the solution.

For spectrophotometric determination of flash-induced H^+ binding the following pH indicator dyes (40 μM) were used (the useful pH range is given in parentheses): bromocresol green (5.0–5.8), chlorophenol red and bromocresol purple (5.8–7.0), phenol red (6.8–8.3), cresol red (7.5–9.6), *m*-cresol purple (7.5–9.5), *o*-cresol phthalein (9.0–10.5), thymol blue (9.0–10.7) and thymol phthalein (10.5–12.0). Before addition of the pH dye, the wavelength of the measuring beam was set to the isosbestic for PQ/P^+Q^- at about 586 nm. The exact location of the isosbestic point depends on the redox state of the reaction center, the addition of inhibitor (terbutryn) and the pH of the solution, as well as on the slit width of the monochromator. Before and after measure-

ment of the flash-induced dye response, the dye was calibrated by addition of aliquots of standard HCl and was corrected for any dilution artifact by mixing the same volume of water. The water calibration was especially important in the alkaline extremum of the indicators, when the solutions were strongly colored and the dye response exhibited low sensitivity. To account for non-bufferable responses at the measuring wavelength, the flash-induced signal was also recorded in the presence of an appropriate hydrogen ion buffer, chosen from Table I, in a final concentration of 10 mM. The degree of buffering was checked by additions of standard HCl and the buffering capacity was explicitly included in calculating the H^+-binding stoichiometry:

$$\frac{H^+}{P^+} = \frac{\frac{V_1}{[P^+]_1} - \frac{V_2}{[P^+]_2}}{S_1 - S_2} \tag{1}$$

where V is the flash-induced response (mV), $[P^+]$ is the amount of flash-induced activation of the reaction centers (μM), S is the sensitivity of the sample (mV per μM HCl) determined by the acid calibrations, and the indexes 1 and 2 refer to the absence and presence of a buffer. The increase in the buffering capacity of the system (S_1/S_2) was generally at least 10.

Since the actinic flashes were more than 97% saturating, the concentration of RCs in a sample was determined by the light-induced absorbance change at 430 nm, using a molar extinction coefficient of 26 $mM^{-1} \cdot cm^{-1}$. This concentration was used as $[P^+]$ in Eq. 1. For the different types of sample, the low level of heterogeneity (less than 10%) in the Q_B content was not normally corrected for. However, a simple correction could be applied for samples with higher residual levels (more than 10%) or less effective reconstitution (less than 90%) of Q_B activity by taking the observed proton binding stoichiometry to be a linear combination of the intrinsic H^+/P^+ stoichiometries of the two types of RCs (completely extracted and fully reconstituted).

For detecting flash-induced pH changes by fluorescence, β-methyl-umbelliferone (100 μM) was added to the sample. The dye was excited at 370 nm and its fluorescence was detected at 490 nm through a broad band blue filter. Net H^+ binding was determined, as above, from the dye responses in unbuffered and buffered samples. The sensitivity of this method is highly influenced by the direct reabsorption of the dye fluorescence by the reaction centers and by the differential absorbance of P/P^+. Thus, the fluorescence transient recorded in the presence of buffer is about 10-times larger than that due to net H^+ binding.

Theory and practice of the conductance-change measurement

Circuit theory

The method is based on an a.c. conductivity bridge which has several advantages: it makes the electrode polarization effects negligible, offers sub-second time resolution and provides a relatively simple correlation between the measured, off-balance, electrical signal and the conductance change evoked by flash excitation. The bridge is driven by a sine wave generator (voltage amplitude V and circular frequency ω) and is balanced before the flash by the variable resistance (R) and capacitance (C) (Fig. 1). Any changes in the conductance (ΔG) or in the capacitance (ΔC) of the measuring cell caused by the flash result in a nonzero difference signal, which can be detected between the points A and B: $v_{AB} = V_A - V_B$. After elementary calculations one obtains:

$$v_{AB} = \frac{V}{4} \frac{\frac{\Delta G}{G} + \left(\frac{\omega C}{G}\right)^2 \frac{\Delta C}{C}}{1 + \left(\frac{\omega C}{G}\right)^2} \tag{2}$$

The capacitance of the cell (C) is kept small (less than 100 pF) by platinizing the Pt electrodes. This decreases the polarizability (Faraday impedance) of the cell and the sine wave suffers no distortion in the vicinity of the balance. The values of G and ω routinely used ($1 \cdot 10^{-3}\ \Omega^{-1}$ and $1.2 \cdot 10^3\ s^{-1}$, respectively) yield $(\omega C/G)^2 \approx 10^{-8} \ll 1$. This allows one to reduce expression (2) to

$$v_{AB} = \frac{V}{4} \frac{\Delta G}{G} \tag{3}$$

Thus, the response of the conductivity bridge is proportional to the flash induced, relative conduc-

tance change of the sample. This a.c. signal is converted into a d.c. signal by the phase- and amplitude-sensitive lock-in amplifier (L). Under our operating conditions (see Eqn. 3), no significant phase shift occurs in the bridge. Consequently, the output of the lock-in amplifier, v, is directly proportional to v_{AB}.

Multiple ionic contributions

The flash-induced conductance change in the solution is attributable to changes in the concentration of mobile ions arising from the uptake and/or release of protons and other ions by the RC in response to the flash. H^+ plays a special role in conductance studies because a variable and often negligible fraction of the hydrogen ions is free, i.e., they are largely buffered. Thus, the conductance changes arising from H^+ binding or release include contributions from correlated changes in the protonation state of any buffer species present. It is assumed that the mobility of the reaction center is negligible compared to that of the smaller ionic species in the solution. The net conductance change can be partitioned into two distinct components:

$$\Delta G_{ion} = \sum_i g_{ion} \frac{I}{P^+}[P^+] \tag{4}$$

$$\Delta G_{H^+} = \sum_{H^+} g_{H^+} \frac{H^+}{P^+}[P^+] \tag{5}$$

The summation of Eqn. 4 should be extended to all ions except hydrogen ions and related hydrogen ion buffers, which are summed in Eqn. 5. I/P^+ and H^+/P^+ are the stoichiometries of ion and proton binding, respectively, and g_{ion} and g_{H^+} are the specific conductances of the non-proton related ions and of protons and proton-carrying species, respectively (see later for a more detailed expression for g_{H^+} in the special case of a cationic buffer). The measured signal is the sum of these components:

$$v_{AB} = v_{ion} + v_{H^+} \tag{6}$$

Using Eqns. 3–5:

$$v_{AB} = \frac{V}{4}\frac{\sum_i g_{ion}}{G}\frac{I}{P^+}[P^+] + \frac{V}{4}\frac{\sum_{H^+} g_{H^+}}{G}\frac{H^+}{P^+}[P^+]$$

or more simply:

$$v_{AB} = \frac{\Delta g_{ion}}{G}[P^+] + S^{H^+}\frac{H^+}{P^+}[P^+] \tag{7}$$

where Δg_{ion} is an effective specific conductance change associated with all ions except those involved in the proton contribution, and S^{H^+} denotes the proton sensitivity of the solution ($\mu V/\mu M$).

The contribution arising from proton binding/unbinding by the RC can be extracted from the total conductance change if the contribution from ions other than protons and proton-buffering species (Δg_{ion}) – the 'non-proton ionic contribution' – is assumed independent of the buffering conditions of the sample. Thus, the difference between two samples of different buffering properties will eliminate any non-proton-related conductance changes. H^+/P^+ can be expressed by directly measurable quantities:

$$\frac{H^+}{P^+} = \frac{\frac{v_1 G_1}{[P^+]} - \frac{v_2 G_2}{[P^+]_2}}{G_1 S_1^{H^+} - G_2 S_2^{H^+}} \tag{8}$$

The indexes 1 and 2 refer to two distinct sample conditions, with different buffering capacities and/or buffer types, as well as possibly different amounts of RCs. Clearly, the larger the difference between the proton sensitivities of the two conditions, the better the resolution of the method. Theoretically, a single buffer species at different concentrations would serve, but a much larger difference can be obtained by applying two buffers of appropriately distinct type (buffer pair). (Table I lists all the buffers used in our experiments.) In response to proton binding by the RC, dipolar (zwitterionic) and anionic buffers will deprotonate generating net charge (negative); thus $S^{H^+} > 0$. The cationic buffers, however, lose net charge if they are deprotonated: $S^{H^+} < 0$. If an appropriate pair of buffers is chosen (e.g., a cationic and a dipolar type), the H^+ contribution to the conductance change will change sign in the two samples. A large enough concentration of buffer must be used to ensure that the protonation events are strongly dominated by the buffer contribution.

The buffer pair method eliminates not only the non-proton ion contributions but also any other

buffer-independent effects. The most important contribution of this type is a heat artifact arising from the flash excitation. The measurement is very sensitive: $\Delta G/G \geqq 0.5 \cdot 10^{-6}$ (typical values: $\omega = 1.2 \cdot 10^3\ s^{-1}$, $V = 1.0$ V, $v_{AB} \geqq 0.1\ \mu$V, $C \leqslant 100$ pF and $G = 1 \cdot 10^{-3}\ \Omega^{-1}$). The heating effect of a single flash is significant and is equivalent to about 10^{-4}–10^{-3} °C temperature rise assuming a temperature coefficient of conductance of 2% per °C [17].

Such a ready diagnostic as the change in sign of the signal in buffer pairs is unfortunately not available for binding or release of ions other than protons. Generally, even the nature of the ion involved in the flash-induced changes is unknown, but it can be calibrated as, e.g., 'chloride equivalent' to yield 'Cl^-/P^+', as for H^+/P^+. In case of negligible heat artifacts, or after suitable correction:

$$\frac{Cl}{P^+} = \frac{v_{AB}}{[P^+]S^{Cl^-}} - \frac{S^{H^+}}{S^{Cl^-}}\frac{H^+}{P^+} \qquad (9)$$

where S^{Cl^-} is the chloride sensitivity of the system (μV/μM); v_{AB} and S^{Cl^-} are measured in the presence of a given buffer and H^+/P^+ is determined from the buffer-pair method.

Sensitivity and selectivity limits

The proton sensitivity of a buffered system is dependent on the pH of the solution. To obtain a simplified expression, let us consider the aqueous solution of a cationic buffer:

$$BH^+ \overset{K_B}{\leftrightarrow} B + H^+$$

$$[BUF] = [B] + [BH^+]$$

The specific conductance arises from charged species:

$$g = zF([BH^+]u_{BH^+} + [H^+]u_{H^+} + [OH^-]u_{OH^-}) \qquad (10)$$

where u denotes the mobility of an ion, F is the Faraday constant and z is the number of elementary charges carried by the ion (here $z = 1$). The proton sensitivity is proportional to the derivative of the conductance change with respect to the H^+ concentration:

$$S^{H^+} \simeq \frac{1}{zF}\frac{\partial g}{\partial [H^+]} \qquad (11)$$

Using Eqn. 10 and introducing the dissociation constants for the buffer (K_B) and for water (K_w),

$$S^{H^+} \approx [BUF]\frac{K_B}{(K_B + [H^+])^2}u_{BH^+} + u_{H^+} - \frac{K_w}{[H^+]^2}u_{OH^-} \qquad (12)$$

For a dipolar buffer, the first term takes a negative sign and the appropriate mobility term is u_{B^-}.

Although u_{H^+} ($3.65 \cdot 10^{-3}$ cm$^2 \cdot$ V$^{-1} \cdot$ s^{-1}, at 25 °C) and u_{OH^-} ($2.05 \cdot 10^{-3}$ cm$^2 \cdot$ V$^{-1} \cdot$ s^{-1}) are much larger than any likely values for u_{BH^+} or u_{B^-}, the contributions of the second and third terms of Eqn. 12 are generally small, due to the low concentrations of free H^+ and OH^-. From the point of view of the buffer pair method it is important for the buffer term (first term in Eqn. 12) to dominate the proton-sensitivity expression. At non-extreme pH values this can easily be fulfilled by using high buffer concentrations and working at pH values close to the pK of the buffer. At very high pH (pH > 11), however, the third term in Eqn. 12 becomes significant and contributes to the proton sensitivity. Changing the buffer type then does not significantly modify the proton sensitivity and the buffer pair method becomes limited.

Calibration

As many different kinds of ions can determine the conductance of a particular sample, an elaborate calibration technique must be applied in order to extract the contribution of hydrogen ions.

The external calibration involves mixing of acid (HCl), salt (NaCl) and water separately. The conductance change caused by adding a definite amount of HCl is due to both the H^+ ions (buffered) and to the Cl^- ions. To determine the Cl^- contribution in the change, NaCl is mixed as a second calibration. Accepting the literature values for the ratio of the mobilities of Cl^- and Na^+ ($u_{Cl^-}/u_{Na^+} = 1.52$) [17], the conductance change attributed to the externally added protons can then be calculated. A water correction is also needed (third calibration) because the volumes added during the acid and salt calibrations cause small (typically $5 \cdot 10^{-4}$) dilutions of the sample, which result in conductance changes comparable

to that of acid or salt additions. Similar procedures can be applied for divalent ion calibration (H_2SO_4 and K_2SO_4).

Results and Discussion

Buffer titration of the conductivity change

To demonstrate that the measured conductivity change is closely related to proton binding by RCs dipolar buffer (glycylglycine) was titrated into a sample containing cationic buffer (Tris) and RCs at constant pH (8.1). The results are summarized in Fig. 2: due to the different nature of the two buffers, the conductivity signal changed sign upon addition of more and more glycylglycine into Tris. However, the contributing proton binding signal, determined by the procedure described above, remained constant over the whole titration range. Although illustrating the point well, the crossover from a negative to positive signal is not located at equimolar concentrations of the two buffers, as one might expect if they were ideally matched. In fact several experimental difficulties contribute to this and prevent a simple quantitative evaluation of the titration curve. The most significant factor arises from the choice of correction for the thermal artifact which, although greatly diminished by the use of a water-filled light guide, was still substantial. Initially, the individual conductivity changes were corrected using the response obtained with no RCs, in Tris buffer. However, this did not account for the heat conversion due to light absorption by the RCs. A more successful correction was obtained by using RCs blocked by over-reduction with dithionite. This can usually be achieved by small additions contributing only about 10% increase in conductivity. Furthermore, the addition of glycylglycine to the solution increases the conductance and, hence, the heat artifact, proportionally. This overly simple correction for the thermal artifact generally overestimates the conductivity change due to proton binding in the presence of glycylglycine.

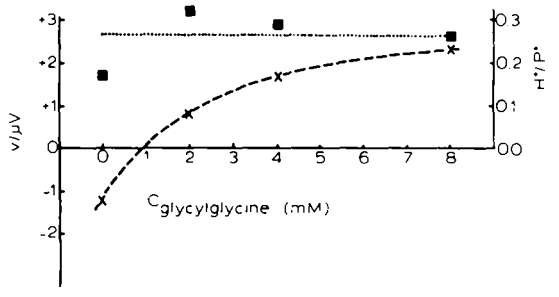

Fig. 2. Amplitude of the flash-induced conductivity change (v; ×) and the amount of proton binding by photoexcited reaction centers (H^+/P^+; ■) as a function of glycylglycine concentration titrated into 4 mM Tris. 0.8 μM reaction centers, 20 μM UQ-10 in 0.03% Triton x-100 (pH = 8.1). Approximately corrected for heat artifact as described in the text.

A further perturbation in this method is an apparent contribution to the signal from non-proton ionic charges following flash excitation. Such contributions will not change sign in the two buffers. The ionic contribution is an increase in conductance, indicating ion release, which diminishes the total signal in Tris buffer but enhances it in glycylglycine. Any differences in the pK values and/or mobilities of the buffers can also modify the shape, or symmetry, of the curve. The transition from negative to positive signal upon titration is obvious, but its exact location is not well determined. The buffer titration clearly demonstrates the involvement of proton binding in the conductivity change, but shows the need for appropriate separation from other ion-related phenomena and for correction for the heat artifact. The buffer-pair method satisfies both requirements.

H^+ binding kinetics

According to the scheme described in the Introduction, the charge-separated state of the RC recombines after flash excitation in the 0.1–1.0 s time range, if no exogenous donor is present. Fig. 3A demonstrates the kinetics of the backreaction measured by the absorbance change at 430 nm at pH 9.8.

Proton binding by RCs is associated with the appearance of an electron on the acceptor side and, therefore, is expected to show similar kinetics to the charge-separation state $P^+(Q_AQ_B)^-$. This is supported by Fig. 3B and 3C. The risetime of the conductance change is very fast (less than 1 ms) and is limited by the time constant of the device (approx. 1 ms). The halftimes for decay of the conductance (245 ± 10 ms) match that of the backreaction (235 ms) very well. The two different types of buffer used show very clearly the change

in direction of H^+ binding. In the case of cationic buffer (2-amino-2-methyl-1-propanol, Fig. 3B) the proton-binding signal is opposite to the direction of the heat artifact (conductance increase), but in the corresponding dipolar buffer (glycine, Fig. 3C same pH 9.8) the two contributions are in the same direction. Separation of the heat artifact is very simple as it is kinetically well distinguished from the H^+ binding signal, and it can be considered as a rectangular pulse on that time scale. The amplitude of the heat artifact was roughly the same in the two samples, as expected, as the conductances were well matched.

The non-proton ionic contribution to the total conductivity change was significant and, because it always appeared as a conductance increase, contributed to differences in the amplitudes of the net conductance change seen in the two types of buffer (compare the different scales of Fig. 3B and 3C). However, it could be successfully eliminated by applying the buffer pair method. A close correspondence between the H^+ binding decay kinetics and the backreaction kinetics was obtained over the whole available pH range (pH 6–11), consistent with the direct involvement of the reduced acceptor side in the H^+ binding by RCs in the absence of exogenous donor.

pH dependence of the first flash H^+ binding in the state P^+Q^-

At any pH, a suitable buffer pair can be chosen from the buffers listed in Table I. Based on Eqn. 8, the absolute value of bound H^+ can be estimated. Fig. 4 shows the pH dependence of the number of protons bound per RC, following a single short flash, in three different cases: Q_B-active, Q_A-active and terbutryn-blocked RCs. All three curves have similar shapes: very low proton uptake at low pH (less than 8), increasing to a maximum at pH 9–10. Although the data are scattered, a decline in H^+ binding at high pH is evident in all cases. The error in the conductimetric H^+-binding measurement at such high pH values is large (indicated by error bars), mainly due to the increasing buffering capacity of the H_2O/OH^- system, which interferes with the sensitivity of the buffer pair method (see Materials and Methods). However, it should be noted that for all pH values above 9.5, where the differences

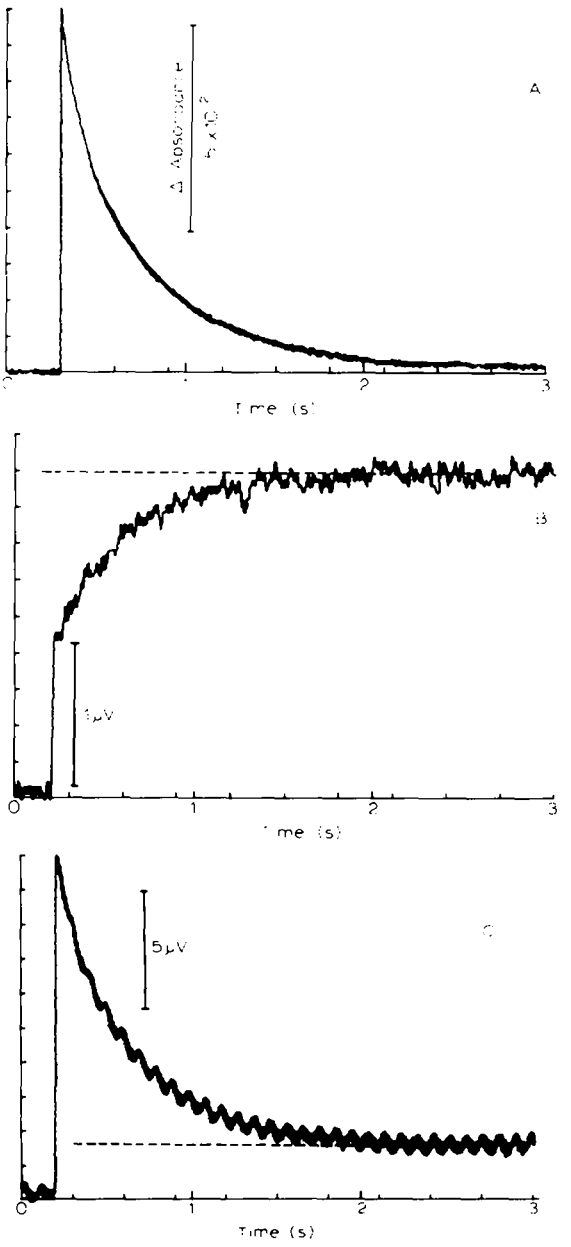

Fig. 3. (A) Flash-induced P^+ kinetics measured at 430 nm. 8 mM glycine, pH = 9.8; 1.2 μM reaction centers, 20 μM UQ-10 in 0.03% Triton X-100. (B) Flash-induced conductivity change at pH 9.8 in 8 mM 2-amino-2-methyl-1-propanol. A proton binding-associated conductivity change is directed downwards. The heat artifact is represented by the stationary value of the total signal. Conditions as for part A, except for buffer; $G = (2304\ \Omega)^{-1}$. (C) Flash-induced conductivity change at pH 9.8 in 8 mM glycine, the buffer-pair of aminomethylpropanol. Proton binding corresponds to an upward deflection and the heat artifact is the stationary value of the decaying signal. Conditions as for part A; $G = (1730\ \Omega)^{-1}$.

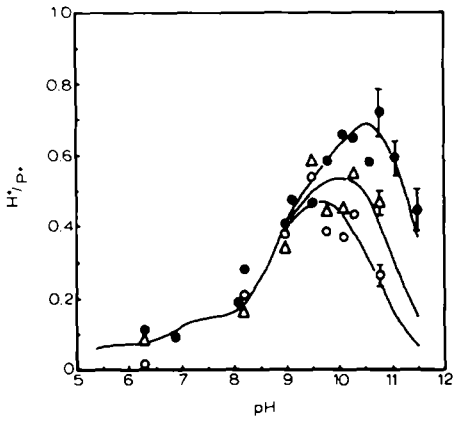

Fig. 4. pH dependence of proton binding by reaction centers, measured by the conductimetric method. The buffer pairs were as follows (see Table I), and were present at a concentration of 8 mM; pH = 6.3, Mes/Bistris; pH = 6.9, Pipes/Bistris propane; pH = 8.1, glycylglycine/Tris; pH = 9.1 and 9.5, Ches/Bistris propane; pH = 9.8, glycine/aminomethylpropanol; pH = 10.1, aspartic acid/ethylenediamine; pH = 10.3, Caps/methylamine + ethylenediamine; pH = 10.8, Caps/methylamine + piperidine. Approx. 1 μM reaction center, 0.03% Triton X-100; Q_B extracted (○), Q_B reconstituted by 20 μM UQ-10 (●), 60 μM terbutryn added (△). The specific proton uptake was calculated from Eqn. 8. Each point at pH 10.8, and higher values, is the average of four determinations; the bars indicate the standard error. The lines were drawn according to the theoretical description in the text – see Table II for pK values.

between the curves become more substantial, the H^+/P^+ ratios decreased in the order: Q_B-reconstituted > Q_B plus terbutryn > Q_A only. At each pH, the three measurements were made on the same sample with sequential additions of ubiquinone (20 μM) and terbutryn (60 μM) to reaction centers largely depleted of Q_B. For each curve, the drop-off in H^+ binding at high pH is well correlated with the redox pK of the quinone species. Although the accuracy of these data does not allow us to conclude exact pK values, approximate pK values can be estimated from Fig. 6: approx. 11.3, for Q_B^- (pK_B), approx. 10.8 for Q_A^- in the presence of terbutryn (pK_T), and approx. 10.5 for Q_A^- only (pK_A). The pK for Q_A samples is somewhat higher than expected from other studies on the redox properties of Q_A, but it is clear that the pK values of the different quinone species lie in the same order (pK_B > pK_T > pK_A) as has been well established by other methods [4,5,8–10]. (The curves in Fig. 4 are drawn as described below.).

Using Eqn. 9 the non-proton ionic contribution to the conductance change could be calculated as the chloride-equivalent anion release by the reaction center. 0.1–0.2 chloride equivalent was unbound per RC, independent of the pH or of the nature of the acceptor quinone species that was active (not shown). Small amounts of ions (Cl^-, Na^+, K^+) are present in the solution, from pH adjustment of the buffers. Replacing these by other ions, such as Mg^{2+}, SO_4^{2-} and tetramethyl ammonium, did not significantly alter the Cl^- equivalent ion release by the reaction center. The insensitivity of the non-protonic conductance change, to the ionic content of the medium, is puzzling. It may imply that this contribution arises from a limited mobility of the reaction center-detergent micelles, but such a contribution should be pH dependent in a manner complementary to that of the net H^+ binding. Possibly the precision of the measurements was insufficient to detect the expected pH dependence. Alternatively, this conductance change component may be only apparent, arising from a systematic error in the complex calibration technique. The actual mobilities of Na^+ and Cl^- are possible sources of this type of error.

Fig. 5 compares the conductimetric data for Q_B-reconstituted RCs with data obtained using

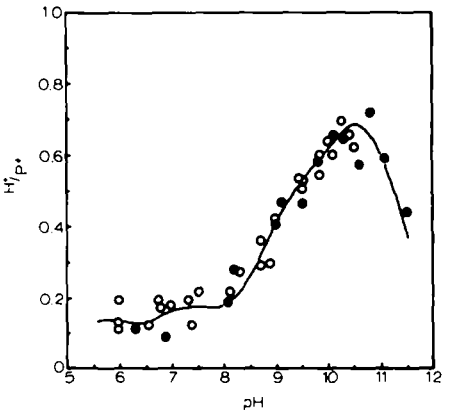

Fig. 5. Comparison of conductimetric and spectrophotometric determinations of H^+-binding by Q_B-reconstituted reaction centers: ●, conductimetric method (data from Fig. 4); ○, spectrophotometric method, using various pH indicators (see Materials and Methods); conditions as for Fig. 4, except plus 10 mM NaCl.

pH-indicator dyes, in the presence of 10 mM NaCl. Some salt was necessary to obtain stable readings of the pH with a glass electrode, and more detailed studies demonstrated that salt concentrations below 20 mM did not have any discernible effect on electron transfer or proton-binding functions of the RC (not shown). The correlation between the spectrophotometric (pH indicators) and conductimetric methods is evidently very good. However, more elaborate studies of H^+ binding using pH indicators were not pursued under low salt conditions because the buffered responses of some dyes were quite large. This seems to arise from an electrochromic effect of the charge separation species (P^+, Q^-) on dye molecules bound to the RC. This response is strongly, but not completely suppressed by higher salt concentrations. In the case of thymol phthalein, the ionic effect of the addition of 10 mM buffer to a low salt medium caused a marked change in the light-induced electrochromic response, thus preventing any quantitative determination of the H^+-binding response. Since thymol phthalein ($pK \approx 11.3$) is the only indicator we have found with adequate sensitivity above pH 10.5, this unfortunate behavior rendered the high pH region inaccessible by the indicator method, under low salt conditions.

It is noteworthy that the pH-indicator data of Fig. 5 were obtained using RCs isolated from the carotenoidless R26 strain as well as from the carotenoid-containing Ga variety of *Rb. sphaeroides*. The results from these two preparations were indistinguishable.

To support further the H^+ binding data obtained here with two distinct methods, a third technique was also applied at low pH: a fluorescent pH indicator, β-methylumbelliferone. In principle this is not entirely different from the measurement of absorption changes of pH indicator dyes but it requires a completely different optical arrangement. The results agreed well with those discussed above: less than 0.1 H^+/P^+ bound at pH 6.62 for Q_B-reaction centers (not shown).

Proton binding in high salt (100 mM NaCl)

The lack of significant H^+ binding at low pH was confirmed, and more extensive data on the proton binding at higher pH could be obtained,

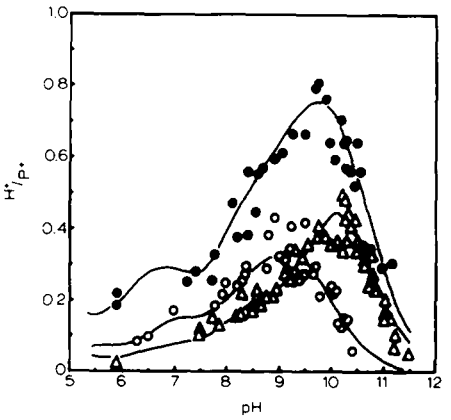

Fig. 6. pH dependence of specific proton binding by reaction centers in high salt, measured by absorbance changes of pH indicator dyes. Approx. 1 μM reaction centers, 0.03% Triton X-100, 100 mM NaCl; Q_B extracted (○), Q_B reconstituted by 20 μM UQ-10 (●), Q_B inhibited by 60 μM terbutryn (△). 40 μM dye (specified in Materials and Methods), was added for measuring the dye response at 586 nm. 10 mM buffer was then added and the buffered baseline signal measured. The curves were drawn as described in the text using the pK values given in Table II.

with pH indicator dyes in high salt medium (100 mM NaCl) (Fig. 6). All pK values appeared to be shifted to lower values, compared to low salt (Fig. 4), as expected for association of positively charged protons with a negative protein. An even more dramatic shift of the pK values was seen in 50 mM $MgCl_2$ (not shown). Also, in high salt, the onset of H^+ binding, as the pH was raised from neutral values, was well separated for the three different states of the acceptor quinone complex. In low salt (Fig. 4) the precision of the conductimetric method was not adequate to indicate whether they were identical or merely close together.

In all cases, for RCs in 100 mM NaCl, the decline in H^+ binding at high pH could be fitted quite well to a Henderson-Hasselbach curve, describing a single protonatable group with a pK corresponding to the known pK value for the reduced form of the relevant acceptor quinone species (Fig. 6)-Q_A^-($pK_A \approx 9.6$), Q_A^-(terbutryn) ($pK_T \approx 10.5$) and Q_B^-($pK_B \approx 10.7$) [4,5,8,9]. The failure of the flash-induced reaction center states, P^+Q^-, to bind protons at lower pH, can be qualitatively explained by supposing that uptake to the semiquinone is masked by proton release from the

P/P^+ couple, as we have previously suggested [18]. This was apparently supported by the partial recovery of H^+ uptake, at low pH, upon reduction of P^+ by donors. One expectation of this model is a transient in the H^+ binding/release kinetics. Since the rate of proton binding is likely to be pH dependent, whereas proton release is expected to be largely pH independent, it should be possible to resolve these two activities, at least in some pH range. However, over the entire pH range where the net proton binding is substantially less than unity, we were unable to detect any indication of a transient H^+ release prior to binding.

Alternatively, the group responsible for the flash-induced proton uptake, at high pH, might be already protonated before the flash, at low pH, i.e., it may exhibit a lower pK in the dark-adapted state. The observed, low levels of proton binding indicate a rather narrow span between the pK values of the oxidized and reduced forms of the quinone, in contrast to equilibrium measurements of the midpoint potentials of Q_A/Q_A^- and Q_B/Q_B^-, which are strongly pH dependent over a wide pH range [8–10]. The difference could arise from the influence of P^+ on the quinone pK values, and this issue is addressed in detail in the accompanying article (Ref. 23).

Within the context of this model, however, the gradual decrease in proton binding, as the pH was lowered below the peak value, cannot be simply described by a single pK on the low pH side of the peak. A single pK on each side would result in a symmetrical pH dependence for the H^+ binding, which would drop to essentially zero at pH values more than one unit on either side of the peak. To describe properly each of the H^+ binding curves of Fig. 6 requires at least six pK values – three promoting H^+ binding as the pH is raised and three suppressing it. In the accompanying article, the H^+ uptake observed in the presence of a donor to P^+, yielding PQ^- as the final state, is shown to be substantially different from that presented here for the P^+Q^-. In order to describe both sets of data, with a minimum number of parameters, it is necessary to invoke eight pK values.

This sudden proliferation of pK values can be made somewhat more palatable when it is recognized that the eight pK values need only represent four ionizable groups subject to differential

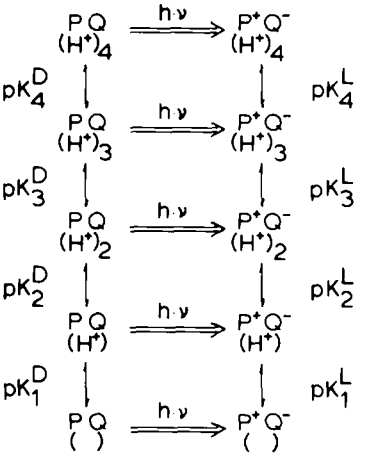

Scheme I.

influences by the redox states of the reaction center; in this case PQ and P^+Q^-. This is shown in Scheme I, although the drawing gives the mistaken impression that the protonation equilibria are sequential. It is more generally expected that the five protonation states within each redox state will be fully connected in a network of equilibria. If the protonation events occur independently, for which we have no evidence for or against, the net proton binding due to each group is described by a bell-shaped curve according to:

$$\frac{H^+}{P^+} = \frac{10^{pK_i^L - pH}}{1+10^{pK_i^L - pH}} - \frac{10^{pK_i^D - pH}}{1+10^{pK_i^D - pH}} \qquad (13)$$

where pK_i^L and pK_i^D are the pK values of the ith group in the P^+Q^- and PQ states, respectively. Each pair of pK values describes a range of pH in which the amplitude of the proton binding to one of the groups is controlled by the span between them – the closer they are the less net proton binding is observed. For four protonatable groups, as shown in Scheme I, the net H^+ uptake is described by the sum of four overlapping curves.

It is actually possible to consider any number of functional (redox-sensitive, protonatable) groups – even a smaller number, if the electrostatic influence of other ionizable groups in the protein is taken into account. Thus, as the net charge on such groups changes with pH, the pK of a nearby redox-sensitive group may also change. However, although interactions of this type are likely, their relevance to the current problem can-

TABLE II

pK VALUES FOR CURVE FITS OF PROTON BINDING (FIGS. 4 AND 6)

Values in parentheses are poorly defined by the available data.

	Q_B				Q_A				+Terb			
	1	2	3	4	1	2	3	4	1	2	3	4
Dark	10.6	8.9	(7.2)	(5.6)	10.0	8.9	(7.2)	(5.6)	10.0	8.9	(7.2)	(5.6)
Light	11.3	9.5	(7.4)	(5.7)	10.5	9.5	(7.4)	(5.7)	10.8	9.5	(7.4)	(5.4)
High salt (100 mM NaCl, Fig. 6) [a]												
	Q_B				Q_A				+Terb			
	1	2	3	4	1	2	3	4	1	2	3	4
Dark	9.1	8.1	6.4	(4.6)	9.2	8.35	6.9	(5.3)	9.7	8.35	6.8	(4.8)
Light	10.6	8.7	6.85	(4.9)	9.65	8.65	7.1	(5.4)	10.5	8.6	6.9	(4.9)

[a] pK values in 100 mM NaCl were obtained from best fits to data in presence and absence of exogenous electron donor to P^+ (see accompanying article: Ref. 23).

not yet be assessed. Furthermore, this view does not offer any additional insights than are available from the original supposition of four separate, redox-sensitive groups. Consideration of a larger number of groups would result in assigning each region of the pH dependence, as described by Eqn. 13, to the combined effects of several groups undergoing proportionally smaller pK shifts. For the time being, it suffices to present the data in the context of four redox-sensitive groups (Scheme I), and the curves drawn in Fig. 6 are based on this description. The pK values are listed in Table II, which also includes the pK values used to fit the low salt data of Figs. 4 and 5. In 100 mM NaCl, the low pK values (in parentheses) are taken from the accompanying article and are included here because they were used to generate the curves shown in Fig. 6. In low salt, the low pK values are poorly defined by the data, but were needed to keep the calculated H^+ binding close to the few data points available at low pH. It should be noted, however, that with a limited number of protonatable groups – such as four – the calculated curve shape is very sensitive to the spacing of all pK values and a change in ΔpK of only 0.1 unit will markedly affect the goodness of fit. The alternative approach is to presume a larger number of groups, all undergoing much smaller pK shifts over a spectrum of median values.

Our failure to detect any transient release of protons upon formation of the P^+Q^- states shows that the two redox centers do not independently affect different subsets of protonatable groups. Clearly the sensitive groups are responding to the redox states of the RC as a whole, i.e., to the net effect of the P^+/P and Q/Q^- redox couples. However, the highest pK in each case does correspond to the known pK value for the reduced form of the relevant acceptor quinone species – Q_A^-, Q_A^-/terbutryn and Q_B^- – implying that P^+P causes little or no perturbance of this ionization equilibrium. Since the next lower pK value is associated with a decline in H^+ uptake as the pH is lowered, it must correspond to the oxidized form of the quinone. The other pK values arise from additional groups under the influence of both P^+/P and Q/Q^- but, with the data from the P^+Q^- only, it is not possible to determine the relative contributions of the two redox couples to the pK shift. This will be addressed in the following article, utilizing data from other redox states of the RC, viz, PQ^- and P^+Q, and further discussion is postponed until then.

Comparison of the methods of pH indicator dyes and of conductivity changes

The original goal of this study was to firmly establish the lack of flash-induced proton uptake by reaction centers at neutral pH. This has now been shown, utilizing two entirely different techniques – spectrophotometric assay with pH-indicating dyes, and conductimetric determination of

changes in mobile charges in the bulk solution, arising from transfer of H^+ between mobile buffers and less mobile reaction center-detergent micelles. The agreement between the two methods is surprisingly good, especially considering the complexity of the calibration procedure for the conductance changes, and we can conclude that there is, indeed, an unexpected failure to observe proton binding to the Q^- species of the reaction center. Comparison of this result with the well-documented pH dependence of the one-electron equilibrium between $Q_A^- Q_B$ and $Q_A Q_B^-$ generates a clear paradox which has been addressed in a preliminary communication [18] and will be elaborated on in the accompanying article.

pH indicator dyes are widely used in proton binding measurements due to their sensitivity and fast response. However, the lack of extensive knowledge of the interactions between reaction center, dye and detergent could make the evaluation of the data difficult. As a result of such interactions, the dye responds, possibly electrochromically, to different redox states of the RC. In principle, this effect can be dealt with by subtracting the response observed after the addition of buffer, but this was only generally reliable in the presence of salt (100 mM) when the addition of buffer did not significantly alter the ionic strength. In this work, with isolated RCs the reference signal could not be identified with that of no added dye, as is often permissible in studies of native membrane systems – chromatophores [19] or chloroplasts [20]. In fact, obtaining an appropriate baseline correction is one of the more serious difficulties in measuring net H^+ binding with pH indicator dyes in isolated RCs because the H^+ binding signal is often not large compared to the background signal. This may be because dye-reaction center interactions allow for substantial electrochromism in the dye molecule in response to charge states of the RC. Furthermore, binding of the dye to the protein or to the detergent micelles can modify the pK of the protonatable group and cause additional difficulties in calibration as the external (acid mixing) calibration occurs in the bulk solution.

The conductimetric method overcomes all of the spectroscopic or related disadvantages of the dye method (overlapping spectral changes of the dye with other components, localized vs. bulk-phase distribution, electrochromism) and preserves its good signal-to-noise ratio, but offers somewhat worse time resolution and, from the present point of view, an inconvenient sensitivity to heat and other ion-related changes. Under appropriate conditions, however, these side effects can be eliminated or significantly reduced and this technique can be a useful tool in studying proton binding/unbinding phenomena evoked by flashes in reaction centers or other light-activated systems. Changes in the non-proton ionic environment can also be monitored, but additional information is required to make quantitative estimates of the stoichiometry of ion binding/release, e.g., identification or determination of the type(s) of ion involved in the change. We have recently learned of Marinetti and Mauzerall's application of both types of measurement to bacteriorhodopsin [21,22].

Acknowledgement

This work has been supported by grants PCM 83-16487 and DMB 86-17144 from the National Science Foundation.

References

1 Crofts, A.R. and Wraight, C.A. (1983) Biochim. Biophys. Acta 726, 149–185.
2 Wraight, C.A. (1979) Biochim. Biophys. Acta 548, 309–327.
3 Wraight, C.A. (1982) in Function of Quinones in Energy Conserving Systems (Trumpower, B.L., ed.), pp. 181–197, Academic Press, New York.
4 Kleinfeld, D., Okamura, M.Y. and Feher, G. (1984) Biochim. Biophys. Acta 766, 126–140.
5 Stein, R.R. (1985) Ph.D. Thesis, University of Illinois, Urbana.
6 Wraight, C.A. and Stein, R.R. (1983) in The Oxygen Evolving System of Photosynthesis (Inoue, Y., Crofts, A.R., Govindjee, Murata, N., Renger, G. and Satoh, K., eds.) pp. 383–392, Academic Press, New York.
7 Wraight, C.A. and Stein, R.R. (1980) FEBS Lett. 113, 73–77.
8 Prince, R.C. and Dutton, P.L. (1976) Arch. Biochem. Biophys. 172, 329–334.
9 Wraight, C.A. (1981) Isr. J. Chem. 21, 348–354.
10 Rutherford, A.W. and Evans, M.C.W. (1980) FEBS Lett. 110, 257–261.
11 Stein, R.R., Castellvi, A.L., Bogacz, J.P. and Wraight, C.A. (1984) J. Cell Biochem. 24, 243–259.
12 Diner, B.A., De Vitry, C. and Schenck, C.C. (1984) Biochim. Biophys. Acta 766, 9–20.

13 Wraight, C.A., Stein, R.R., Shopes, R.J. and McComb, J.C. (1984) in Advances in Photosynthesis Research (Sybesma, C., ed.), Vol. I, pp. 629–636, Martinus Nijhoff/Dr. W. Junk Publishers, Dordrecht.
14 Maróti, P. and Wraight, C.A. (1985) Biophys. J. 47, 536a.
15 Marinetti, T. (1984) Biophys. J. 45, 217a.
16 Okamura, M.Y., Isaacson, R.A. and Feher, G. (1975) Proc. Natl. Acad. Sci. USA 72, 3491–3495.
17 Daniels, F. and Alberty, R.A. (1967) Physical Chemistry, p. 399, John Wiley, New York.
18 Maróti, P. and Wraight, C.A. (1986) in Progress in Photosynthesis Research (Biggins, J., ed.), Vol. II, pp. 401–404, Martinus Nijhoff, Dordrecht.
19 Petty, K.M., Jackson, J.D. and Dutton, P.L. (1979) Biochim. Biophys. Acta 546, 17–42.
20 Junge, W. and Ausländer, W. (1973) Biochim. Biophys. Acta 333, 59–70.
21 Marinetti, T. and Mauzerall, D. (1983) Proc. Natl. Acad. Sci. USA 80, 178–180.
22 Marinetti, T. and Mauzerall, D. (1986) Biophys. J. 50, 405–415.
23 Maróti, P. and Wraight, C.A. (1988) Biochim. Biophys. Acta 934, 329–347.